



UNIVERSITY OF LEEDS

This is a repository copy of *Conformational Space and Stability of ETD Charge Reduction Products of Ubiquitin*.

White Rose Research Online URL for this paper:
<http://eprints.whiterose.ac.uk/105282/>

Version: Accepted Version

Article:

Lermyte, F, Łacki, MK, Valkenborg, D et al. (2 more authors) (2017) Conformational Space and Stability of ETD Charge Reduction Products of Ubiquitin. *Journal of the American Society for Mass Spectrometry*, 28 (1). pp. 69-76. ISSN 1044-0305

<https://doi.org/10.1007/s13361-016-1444-7>

© 2016, American Society for Mass Spectrometry. This is an author produced version of a paper published in *Journal of The American Society for Mass Spectrometry*. The final publication is available at Springer via <https://doi.org/10.1007/s13361-016-1444-7>.
Uploaded in accordance with the publisher's self-archiving policy.

Reuse

Unless indicated otherwise, fulltext items are protected by copyright with all rights reserved. The copyright exception in section 29 of the Copyright, Designs and Patents Act 1988 allows the making of a single copy solely for the purpose of non-commercial research or private study within the limits of fair dealing. The publisher or other rights-holder may allow further reproduction and re-use of this version - refer to the White Rose Research Online record for this item. Where records identify the publisher as the copyright holder, users can verify any specific terms of use on the publisher's website.

Takedown

If you consider content in White Rose Research Online to be in breach of UK law, please notify us by emailing eprints@whiterose.ac.uk including the URL of the record and the reason for the withdrawal request.



eprints@whiterose.ac.uk
<https://eprints.whiterose.ac.uk/>

Conformational space and stability of ETD charge reduction products of ubiquitin

Frederik Lermyte^{1,2}, Mateusz Krzysztof Łacki³, Dirk Valkenborg^{2,4,5}, Anna Gambin³, Frank Sobott^{1,6,7}

¹Biomolecular & Analytical Mass Spectrometry Group, Department of Chemistry, University of Antwerp, Antwerpen, Belgium

²Center for Proteomics, University of Antwerp, Antwerpen, Belgium

³Institute of Informatics, University of Warsaw, Poland

⁴Interuniversity Institute for Biostatistics and Statistical Bioinformatics, Hasselt University, Belgium

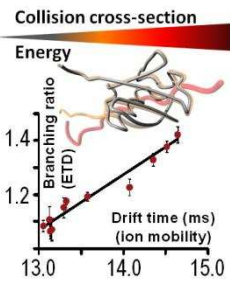
⁵Applied Bio & Molecular Systems, Flemish Institute for Technological Research (VITO), Belgium

⁶Astbury Centre for Structural Molecular Biology, University of Leeds, Leeds LS2 9JT, United Kingdom

⁷School of Molecular and Cellular Biology, University of Leeds, LS2 9JT, United Kingdom

Abstract

Due to its versatility, electron transfer dissociation (ETD) has become one of the most commonly utilized fragmentation techniques in both native and non-native top-down mass spectrometry. However, several competing reactions – primarily different forms of charge reduction – occur under ETD conditions, as evidenced by the distorted isotope patterns usually observed. In this work, we analyze these isotope patterns to compare the stability of ETnoD products, specifically noncovalent *c/z* fragment complexes, across a range of ubiquitin conformational states. Using ion mobility, we find that more extended states are more prone to fragment release. We obtain evidence that for a given charge state, populations of ubiquitin ions formed either directly by electrospray ionization or through collapse of more extended states upon charge reduction, span a similar range of collision cross-sections. Products of gas-phase collapse are however less stabilized towards unfolding than the native conformation, indicating that the ions retain a memory of previous conformational states. Furthermore, this collapse of charge-reduced ions is promoted if the ions are ‘pre-heated’ using collisional activation, with possible implications for the kinetics of gas-phase compaction.



Address reprint requests to: frank.sobott@uantwerpen.be

Running title: Conformational space of ubiquitin in crETD

Introduction

In the past decade, electron transfer dissociation (ETD)[1] has been implemented in a variety of commercially available mass spectrometers, and has become increasingly important in top-down protein analysis under both native and denaturing conditions[2]. The main reason for this is the ability of ETD to induce backbone cleavage while preserving weak bonds, particularly noncovalent interactions. Multiple ion/ion reaction pathways are available under ETD conditions, including several forms of non-dissociative charge reduction (see Figure 1)[3-6], for which we introduced the term charge-reduction ETD (crETD). The most important contributions to crETD are non-dissociative electron transfer (ETnoD) and the proton transfer reaction (PTR). The third charge reduction channel, gas-phase adduction of a reagent anion, is typically sufficiently rare so that it can be disregarded. As before[7], we note that electron transfer followed by loss of a hydrogen atom by the protein, which has been proposed to occur to some extent in hypervalent ammonium radicals under ECD conditions[8-11], is not explicitly included in our approach, but contributes to the intensity of the PTR channel.

PTR of an ESI-generated $[M+nH]^{n+}$ precursor leads to an even-electron $[M+(n-1)H]^{(n-1)+}$ product, whereas ETnoD of the same precursor leads to an $[M+nH]^{(n-1)+\bullet}$ radical. Two types of such radicals exist: In the first, backbone cleavage occurred, but the resulting *c* and *z* fragments are held together by noncovalent interactions; in the second, the electron is accommodated e.g. in an aromatic side chain, and its presence does not lead to backbone cleavage. As they possess the same molecular formula, i.e. $[M+nH]^{(n-1)+\bullet}$, distinction of both types of ETnoD ion by mass alone is impossible. Upon application of supplemental (collisional) activation, however, the noncovalent interactions stabilizing the first type of ETnoD product are disrupted, leading to the release of *c* and *z* fragments. The second type, on the other hand, will not readily dissociate upon application of supplemental activation and will form only CID-type (*b* and *y*) ions when sufficiently activated[2]. The actual branching ratio between transfer of either a proton or electron during ion/ion interaction is believed to be mainly a function of properties of the reagent anion[12, 13]. We therefore assume this ratio to be constant for a given reagent, as well as the protein, its charge state, and conformation. For a structurally heterogeneous protein, it is conceivable that different conformations might have different reactivities toward proton and electron transfer, due to e.g. different degrees of electrostatic repulsion or intramolecular proton solvation. Indeed, it has been proposed by Clemmer and colleagues[14] that significantly different conformations (i.e. 20 – 50% difference in collision cross-section) of ubiquitin possess different reactivities in ion/neutral proton transfer, although Smith and colleagues have argued that any such effect is fairly minor[15]. For the fairly homogeneous, extended conformations used in our experiments, however, our assumption – that subtle conformational differences within the highly charged states which we observe do not have a major effect on ion/ion reactivity – seems plausible. It is important to note that the ‘apparent’ PTR/ETnoD branching ratio referred to in this work is the observed ratio based on ions which survive long enough to be detected. Crucially, we assume that virtually all PTR products will be detected (since these are stable), while the population of ETnoD ions will be depleted – and the observed branching ratio thus distorted – to some extent by conversion into ETD fragments.

As PTR and ETnoD products differ by one hydrogen mass, they can in principle be distinguished relatively easily. In practice, however, both pathways co-exist, leading (especially after multiple reaction steps) to complex signals which consist of several overlapping isotope distributions.

Recently, we have presented software which, based on the precursor sequence and charge state, predicts the isotope distributions of all possible products (accounting for multiple reaction steps), and subsequently ‘deconvolutes’ ETD spectra, thereby yielding the relative intensity of each product[7]. The intensities of the different types of products were shown to be sensitive to application of supplemental activation, in a manner which was easily rationalized through collision-induced dissociation of noncovalent *c/z* fragment complexes.

In the current work, using gentle ESI and the ion mobility (IM) capabilities of the Synapt G2 HDMS instrument, we investigate the relation between the apparent preference for either type of charge reduction – which, as mentioned, is assumed to depend mostly on survival of ETnoD products – and the collision cross-section (CCS) of the precursor and charge-reduced products. Further, we also study how this relation depends on the application of limited collisional activation (both pre- and post-ETD; before the ions enter the IM cell in each case). By varying acceleration voltages, we generate extended and (partially) collapsed drift-time species for 6+ ubiquitin, formed by charge reduction of the ESI-generated $[M+8H]^{8+}$ precursor, and compare these to $[M+6H]^{6+}$ ions directly generated by ESI. Regardless of the stage at which collisional activation was applied, a good correlation between average drift time (compactness) and apparent PTR/ETnoD branching ratio was found. This can be rationalized as the more compact structures of *c/z* complexes are stabilized to a greater degree by noncovalent interactions, even though they are formed by gas-phase collapse of more highly charged, extended structures on a millisecond timescale. This results in a reduced propensity for fragment release and more ETnoD ions reaching the detector, decreasing the observed PTR/ETnoD ratio. As such, this method, which can be applied to any high-resolution, ETD-capable mass spectrometer, provides a new way of gaining insight into the global structure and dynamics of gas-phase protein ions.

Experimental

The MassTodon software used to analyze observed isotope distributions was developed in-house and described previously[7]. CCS calibration was performed using a standard protocol[16], but taking reference values for denatured ubiquitin from a more recent report[17]. Experiments were carried out on an ETD-capable hybrid quadrupole/ion mobility/time-of-flight mass spectrometer (Synapt G2 HDMS, Waters, Wilmslow, UK). Ubiquitin (Sigma U6253, 8564.8 Da) was used at a concentration of 5 μ M in water/methanol (v/v) 50/50 with 0.1% formic acid added. The sample was introduced using nano-ESI via in-house prepared gold-coated glass capillaries, using a spray voltage of 1.0 kV and 0.20 mbar nanoflow gas pressure. The glow discharge was tuned to provide an ETD reagent (1,4-dicyanobenzene) current of approximately $2e6$ counts/s for charge reduction, and was switched off to measure drift times of ESI-generated ions. Anions were accumulated in the trap T-Wave cell for 100 ms with a refill interval of 1 s. Backing and source pressure were $2.8e0$ and $1.8e-3$ mbar, respectively. Sampling cone and trap DC bias were varied as described in the text. An outline of the instrument is shown in Supplementary Figure S-1. Pressure in the trap, He, IM, and transfer cell were $7.4e-2$ (gas flow 20 mL/min), $1.4e3$ (140 mL/min), $2.5e0$ (60 mL/min), and $3.7e-2$ (4 mL/min) mbar, respectively. Standard values for IM wave height and velocity were 20 V and 500 m/s, respectively.

To allow for more accurate determination of CCS values of ESI-generated ubiquitin charge states 4+ to 7+, additional experiments using IM wave height/velocity of 25 V / 700 m/s and 30 V / 1000 m/s

were performed. Since the aim of this work was to induce limited charge reduction rather than maximize fragmentation, the trap wave height, which controls the extent of ion/ion interaction[18, 19], was kept relatively high, at 1.2 V. Trap wave velocity was 300 m/s.

A minimum of three repeats were performed for all charge reduction experiments, and average branching ratios are reported. The method for estimating separate (apparent) branching ratios for both reaction steps is described in the Supplementary Information. Data processing was performed using both MassLynx (version 4.1) and the in-house developed MassTodon software. External m/z calibration was performed using cesium iodide clusters.

Results and Discussion

Previously, we compared the ETD fragmentation behavior of native and partially unfolded structures of large noncovalent complexes[20]. Partial unfolding in this case was induced prior to ETD and confirmed using IM. Fragment release from the fully folded complexes was found to require significant supplemental activation (applied in the transfer cell) in nearly all cases. For partially unfolded species on the other hand, fragments were released immediately after electron transfer (also confirmed using IM), without applying supplemental activation. Partially unfolded species release fragments more readily, due to a reduced presence of hydrogen bonds and salt bridges. Accordingly, this should deplete the ETnoD products, resulting in an apparent increase in PTR/ETnoD branching ratios. In the current work, we investigate whether a correlation exists between this branching ratio of a (charge-reduced) precursor and its arrival time in IM.

The MassTodon software, which we developed previously for estimating this ratio, requires that isotopes of charge-reduced products be resolved, which is difficult in native ESI of large protein complexes[21]. We therefore focused our investigation on ubiquitin, a small (8.6 kDa), well-characterized monomeric protein. Ubiquitin is known to adopt various conformations in the gas phase, particularly at intermediate charge states[14, 22, 23]. It was recently shown that the relative abundances of these conformations result at least in part from gas-phase activation[24]. Thus, we decided to systematically vary the sampling cone (activating the 8+ ESI-generated ion) and trap DC bias (activating the 6+ charge-reduced product) voltages under ETD conditions, whilst isolating the $[M+8H]^{8+}$ ion in the quadrupole. The relative location where these potentials are applied within the instrument can be found in Supplementary Figure S-1. It should be noted that the cone voltage is applied before and the bias voltage after ETD, while both are applied prior to the IM cell. For each set of parameters, a minimum of three spectra was acquired and the PTR/ETnoD branching ratio calculated for each spectrum. The branching ratio for the first reaction step ($8+ \rightarrow 7+$) is simply the ratio of the detected amount of PTR ($[M+7H]^{7+}$) and ETnoD ($[M+8H]^{7+\bullet}$) product and was consistently between 1.082 and 1.122 ($\pm 1.8\%$ variability). The observed CCS distributions for the 7+ charge state (See Supplementary Figure S-2) are also nearly identical between experiments. Maximum likelihood estimation subsequently allowed determination of the apparent branching ratio for the second step ($7+ \rightarrow 6+$) separately, based on the ratio observed in the first step and the amounts of '2 x PTR', '2 x ETnoD', and 'hybrid' product that combine to make up the observed 6+ species (See Supplementary Information). Interestingly, this second branching ratio varied between 1.066 and 1.423 ($\pm 16.7\%$ variability), reflecting the much greater structural heterogeneity of the 6+ charge state.

Assuming – as we will later show to be true – that gas-phase unfolding and collapse lead to a small number of quite well-defined conformations, the CCS distribution of the 6+ charge-reduced ion can be meaningfully represented as a (weighted) average of these states. In Figure 2a, the apparent (7+ → 6+) PTR/ETnoD branching ratio is plotted as a function of the weighted average of the CCS values of charge-reduced 6+ ions across all experiments. The observed isotope distribution of this ion in two of the spectra (i.e. two of the eleven data points in Figure 2a) is shown in Figure 2b, demonstrating that a deviation from the $[M+6H]^{6+}$ ion generated by ESI is clearly visible even upon casual inspection. Two features of Figure 2a are striking: First of all, the quasi-linear trend is consistent with our hypothesis that more extended conformations are more likely to release fragments and therefore exhibit a higher branching ratio (less ETnoD surviving). Second of all, charge-reduced ions generated after cone activation are on average more compact than those generated by bias activation.

In the following, we will look at the CCS distributions of the various charge(-reduced) states of ubiquitin in more detail. While charge reduction in the gas or droplet phase via ion/ion and ion/neutral chemistry has been performed before, the focus was on spectral simplification or deconvolution of overlapping signals in the m/z domain, rather than investigating the effect on gas-phase ion structure[4, 6, 25-28]. Efforts to combine this approach with ion mobility have mostly focused on large, noncovalent complexes, and in these cases, little or no conformational change has generally been observed[5, 29-31].

Figure 3 shows CCS distributions of 6+ ubiquitin, generated either directly by ESI (panels a-b), or by double gas-phase charge reduction of the ESI-generated $[M+8H]^{8+}$ precursor (panels c-d). In Figure 3a, it can be seen that the trap DC bias voltage has a profound effect on the CCS distribution of the ESI-generated $[M+6H]^{6+}$ ion: When this voltage is increased from 25 to 45 V, the protein fully converts from a conformation with a collision cross-section (CCS) of ca. 1560 Å² to a more extended form with a CCS of around 1830 Å² (+17%), with both conformations coexisting at intermediate bias voltages. Similar behavior occurs with increasing sampling cone (Figure 3b), but an intermediate conformation with a CCS around 1730 Å² is also observed, most likely due to the presence of residual solvent on the protein at this early stage of the ion transfer into vacuum. Charge states 7+ and 8+ show only the extended conformation (Supplementary Figure S-2).

Our CCS values are larger than reported in a recent study[24]; however, that study used an IM calibration protocol[16] which relies on reference values measured in helium by the Clemmer group[14]. A reasonably good correlation is known to exist between CCS values measured in He and N₂, particularly for peptides of the same charge state[16, 17, 32]. A comparison of reference values for different charge states of denatured ubiquitin obtained from a linear IM cell in both gases[14, 17] shows, however, not only that nitrogen values are systematically larger, but also reveals a much greater increase of CCS with charge in this gas, likely due to its greater polarizability[33]. Using the Clemmer CCS values for denatured ubiquitin (in helium) to calibrate our IM data, we obtain values for the 1560, 1730, and 1830 Å² species which are 15-20% smaller (1280, 1460, and 1580 Å², respectively). This matches what is referred to as the I(ntermediate) (ca. 1200 Å²), E(xtended)-2 (ca. 1400 Å²), and E(xtended)-1 (ca. 1500 Å²) states in [24]. At the bottom of each panel in Figure 3, the lowest-energy (blue) CCS distribution is represented by a linear combination of these three (Gaussian) components. The fact that all twelve traces in Figure 3 can be adequately described as such linear combinations (Supplementary Figure S-3) validates our assumption of a small number of gas-phase conformations, for both ESI-generated and charge-reduced 6+ ubiquitin ions.

As CCS values for the C(ompact) state of ubiquitin (charge states below 7+) in N₂ are not found in the most commonly used databases (i.e. those hosted by the Clemmer and Bush groups), we can report here that we find values of (1264±17), (1240±18), and (1231±20) Å² for the 6+, 5+ and 4+ ESI-generated ions, respectively. Matching our other results, these values are again ca. 20% higher than reference values (ca. 1050 Å²) measured in helium[14, 34]. For the 6+ ion, this state was only observed if the sampling and extraction cone voltages were significantly lowered, to 8 V (minimum for ion transmission) and 1 V, respectively. Only the *I*, *E1*, and *E2* states contribute significantly to the CCS distributions shown in Figure 3.

Figure 3c shows that the extended 8+ ion (ca. 2000 Å², Supplementary Figure S-2e,f) collapses upon charge reduction to 6+. The resulting ion population spans the same CCS range as the ESI-generated [M+6H]⁶⁺ ion, but is largely trapped in intermediate states in the absence of post-ETD activation (blue trace). The fact that the more compact conformations are not observed in charge states above 6+ indicates that they are indeed formed by charge-driven gas-phase collapse rather than already being present in the quadrupole-selected 8+ precursor and merely undergoing charge reduction more efficiently than the extended conformers. This further supports our hypothesis that subtle conformational effects do not play a major role in determining the actual ion/ion reactivity. The relatively compact *I* state at ca. 1560 Å², which survives moderate activation in the ESI-generated 6+ ion (Figure 3a, orange trace), is absent in the charge-reduced case (Figure 3c, orange trace). This indicates that charge-induced compaction may well lead to structures of similar CCS, but with reduced stability towards unfolding compared to the ESI-generated structure (while 40 V of cone voltage correspond to higher activation for the 8+ precursor than the 6+ ESI ion, we expect the ions to be largely thermalized again by the time the ions reach the trap cell).

A sufficient increase in bias voltage produces in both cases virtually identical CCS distributions, which represent extended conformations (red traces in Figure 3a,c). An increased cone voltage on the other hand (Figure 3d) leads to significant heterogeneity for the charge-reduced product at all cone voltages in the 40-100 V range, with a predominance of compact conformations. It appears that the structure of the 8+ precursor is already sufficiently disrupted, and the resulting extended form stabilized by charging, so that cone activation does not have any significant effect (Supplementary Figure S-2f,h). Consequently, the 6+ crETD products of this 8+ precursor also show similar CCS distributions, apart from a slight shift towards more compact states at higher cone voltages (Figure 3d). Possibly, the increased internal energy of the [M+8H]⁸⁺ ions during desolvation disrupts some H-bonds and salt bridges, leading to an extended conformation which has a low barrier for collapse due to charge reduction. It should be noted however, that although the entire ESI-generated ion population undergoes collisional activation due to an increased cone voltage, only the [M+8H]⁸⁺ ion is selected in the quadrupole and allowed to interact with the anions in the trap cell.

The data presented so far are in agreement with the observed correlation between different arrival time distributions, characterized by average CCS values, and the extent of fragment release, reported as an apparent PTR/ETnoD branching ratio in Figure 2. It is conceivable however that the competing ETnoD and PTR reactions could lead to charge-reduced products with subtly different conformations, and that ion activation somehow biases the ratio between electron and proton transfer. However, it is counter-intuitive that transfer of either an electron or a proton would lead to such large CCS differences as observed in Figure 3. Additionally, both we and others have shown previously[7, 23, 35] that charge reduction of high charge states of ubiquitin, using the PTR-specific reagent PDCH

(perfluoro-1,3-dimethylcyclohexane), leads to the same conformational heterogeneity for the 6+ ion as observed here. Similar results were also observed by Badman and colleagues for cytochrome c[36], although they speculated that the intermediate and compact conformations formed by charge reduction of extended, highly charged ions, were the result of refolding to similar conformations as those generated by ESI, whereas our results suggest a different pattern of noncovalent stabilizing interactions (i.e. salt bridges) Finally, while activation at the cone (i.e. before ETD) could theoretically change the preference for initial proton or electron transfer, for the bias voltage (downstream of the ETD cell) to affect the apparent PTR/ETnoD ratio, the same argument of “depletion by fragmentation” would have to be made as in our model.

Rather than our hypothesis that gas-phase activation induces a structural change, with different conformations subsequently generated possessing different propensities for fragment release from noncovalent *c/z* fragment complexes, it could also be proposed that the change in CCS distributions observed in Figure 3c,d is the result of certain conformations being selectively depleted by dissociation. In Figure 3c, this would mean conversion of the more compact conformations to ETD fragments with increasing bias voltage, while leaving the more extended conformations largely unaffected. However, first of all, total conversion of ETnoD products to ETD fragments does not occur at the low activation voltages used here (particularly as the trap gas in this case is helium). Secondly, this would imply that the more compact conformation consists nearly exclusively of ETnoD product, which we have already ruled out in the previous paragraph. A similar argument can be made for why Figure 3d likely also shows mainly conformational transitions rather than the effect of selective dissociation.

Having said this, it should be noted that some minor distortion of the observed CCS distributions is inevitable within our model, as by definition, we detect only the surviving ions and not the initially formed ion population. As survival rate differs between conformations, we expect that we underestimate the average arrival time somewhat, particularly for ion populations in which a significant portion occurs as extended conformations. However, this distortion is expected to be quite small for several reasons: First of all, a significant amount of PTR product is present, which does not fragment and for which we therefore do actually detect the initially formed population. Secondly, even for the most extended conformation of 6+ ubiquitin we observe that our data are consistent with dissociation of only a minority of the ETnoD ions. As such, while an increased abundance of extended conformation(s) might be attenuated somewhat by this effect, it will still be clearly visible in our data.

As mentioned, the collapsed *I* state we observe is clearly less stable toward collision-induced unfolding than the similarly-sized ESI-generated $[M+6H]^{6+}$ ion, as demonstrated by the complete depletion of this state with a minor increase in bias voltage. Interestingly, however, the apparent PTR/ETnoD branching ratios can be predicted (based on the deconvolution into Gaussian components) with an error of less than 5% (even less than 1% in most cases) across all experiments if one assumes that only the *I*, *E2*, and *E1* states occur, and that these exhibit branching ratios of 0.797, 1.076, and 1.479 respectively. This indicates that, despite reduced stability compared to the ESI-generated ion, hydrogen bond and salt bridge formation during collapse make the compacted ion significantly more capable than the extended state of forming long-lived *c/z* fragment complexes. A possible explanation for this is that during collapse, groups with a tendency to form noncovalent contacts (e.g. charged groups) easily find interaction partners locally, without the global fold of the

protein being stabilized to a similar degree as in the native structure. This is in excellent agreement with results which were reported recently by Vachet and colleagues[37], who performed ETD in a quadrupole ion trap. This phenomenon could perhaps even provide insight into why, using ECD on FTICR instruments (somewhat harsh interface, ion residence time up to seconds), a rearrangement to a compact, salt-bridge stabilized, yet distinctly non-native structure is consistently reported when spraying ubiquitin from either acidified water/methanol solution[38], or native-like aqueous ammonium acetate[39].

These previous studies focused on the ExD fragmentation pattern of ubiquitin in order to infer structural information for the precursor, which was isolated in the quadrupole. Crucially, relatively low (< 7+) charge states were typically selected, occurring (according to our IM data as well as that of others[14, 16, 24]) in compact and intermediate conformations and resulting in a lack of observed fragmentation in certain regions – mostly those spanned by salt bridges. Conversely, in our work, both the 8+ precursor isolated in the quadrupole, as well as the first (7+) charge-reduced state, occur fully in the extended state (Supplementary Figure S-2). Intensity ratios of the (ESI-generated) 8+, (charge-reduced) 7+, and (charge-reduced) 6+ states of ‘intact’ ubiquitin in our crETD spectra are around 20:5:1 (see Supplementary Figure S-4) – in agreement with the exponential decrease expected from reaction kinetics. Therefore, the majority of the fragments originate from extended conformations. Since both ETD and collisional activation in our experiments occurred prior to entry of the ions into the ion mobility cell, distinguishing fragments released from the 6+ state by drift time alignment was obviously also not possible. As mentioned, instrument conditions were optimized for (limited) charge reduction rather than high fragmentation efficiency, and as a result, the intensities of even the most abundant fragments were another order of magnitude less than those of even the 6+ charge reduction products. As such, the changes in intensities of individual fragments - due to changing propensity for fragment release from the 6+ charge-reduced state - are too small to be monitored with the same reliability as using our IM and isotope distribution analysis. However, it is still possible to estimate total fragment intensity in a consistent manner. Doing this for all our spectra, we observe that the relative total fragment intensity observed in our experiments follows a similar trend as the apparent PTR/ETnoD ratio (Supplementary Figure S-5). This is in agreement with our hypothesis that fragment release is the dominant factor determining apparent PTR/ETnoD ratio.

A recent report showed a range of biologically irrelevant compact (collapsed) subpopulations in ‘native’ IM-MS of several intrinsically disordered proteins[40]. Another study demonstrated a dramatic change in CCS of ubiquitin, cytochrome c, and myoglobin at intermediate charge states after noncovalent binding of a 264 Da crown ether ligand[41]. In this case, inhibiting the collapse of a single charge site onto the backbone was sufficient to prevent a much more dramatic disruption of the native hydrogen bond network and subsequent unfolding of these ‘frustrated’ (i.e. electrostatic repulsion being barely canceled out by noncovalent stabilization) ions. Such studies, as well as our own results presented here, serve as a reminder that experimental determinants of ‘native’ conditions in MS need to be carefully examined. This is particularly true for small proteins, as these possess a comparatively high number of charges relative to the number and strength of noncovalent interactions stabilizing the native structure. As such, the occurrence of charge-driven processes is facilitated, potentially muddying the relation between structure in solution and in the gas phase.

Conclusion

We have explored the conformational space occupied by ubiquitin during charge reduction ETD (crETD). The resulting (collapsed) states span the same range of collision cross-section values as ions of the same charge state generated directly by electrospray ionization; however, collapsed states are generally less stable toward collision-induced unfolding than the solution structure. Furthermore, we have described a method of estimating apparent branching ratios for competing reaction pathways under ETD conditions. Due to conformation-dependent depletion of noncovalent ETD fragment complexes, this ratio is strongly dependent on gas-phase ion structure, and a clear correlation with arrival time in ion mobility exists. This correlation indicates that, despite the limited stability of collapsed ions, 'local' stabilizing interactions, leading to increased preservation of fragment complexes, are more prevalent in these compact states than extended ones. The observation that in-source ion activation leads to increased collapse following charge reduction is surprising, and more in-depth work on the kinetics of charge-driven gas-phase refolding will be the focus of future research.

Acknowledgements

We thank the Research Foundation – Flanders (FWO) for funding a PhD fellowship (F.L.). The Synapt G2 mass spectrometer is funded by a grant from the Hercules Foundation – Flanders. This work is in part supported by Polish NCN grants No. 2014/12/W/ST5/00592 and 2015/17/N/ST6/03565. We thank the reviewers for their valuable comments.

Figures

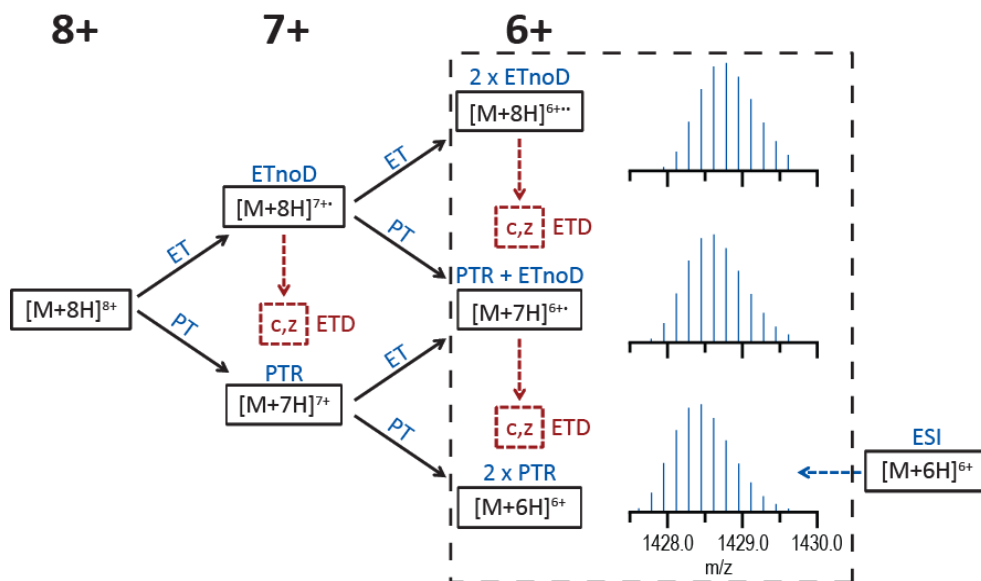


Figure 1. Reaction pathways in double charge reduction of (ESI-generated) $[M+8H]^{8+}$ ubiquitin. Ions of 'intact' ubiquitin, i.e. precursor and products of charge reduction, are shown in black, while ion/ion reactions are shown in blue. Dissociation into *c* and *z* fragments (shown in red) can only occur for radical species (not for 'pure' PTR products), leading to depletion of these species and an increase in apparent PTR/ETnoD ratio.

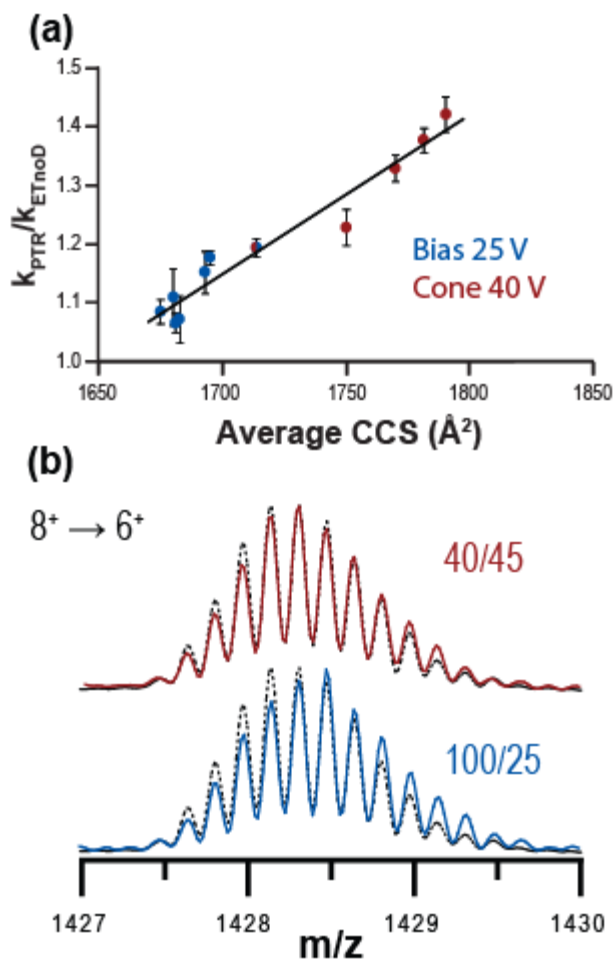


Figure 2. (a) Apparent PTR/ETnoD branching ratio for the second (i.e. $7+ \rightarrow 6+$) charge reduction step ($[M+8H]^{8+}$ precursor selected in the quadrupole) versus average collision cross-section for the corresponding $6+$ charge-reduced state. Blue dots indicate experiments in which the bias voltage was held constant at 25 V (varied sampling cone voltage); red dots indicate a constant cone voltage of 40 V, with variable trap DC bias. (b) Isotope distributions for the $6+$ charge-reduced product acquired with (blue) a sampling cone of 100 V and a trap DC bias of 25 V, or (red) a cone of 40 V and a bias of 45 V. The dashed line shows the isotope distribution of the $[M+6H]^{6+}$ ion generated by ESI, corresponding to an 'infinite' PTR/ETnoD branching ratio. Note that the red trace approaches the dashed line more closely than the blue trace (i.e. higher percentage of ESI-like ions), in agreement with the plot shown in panel (a).

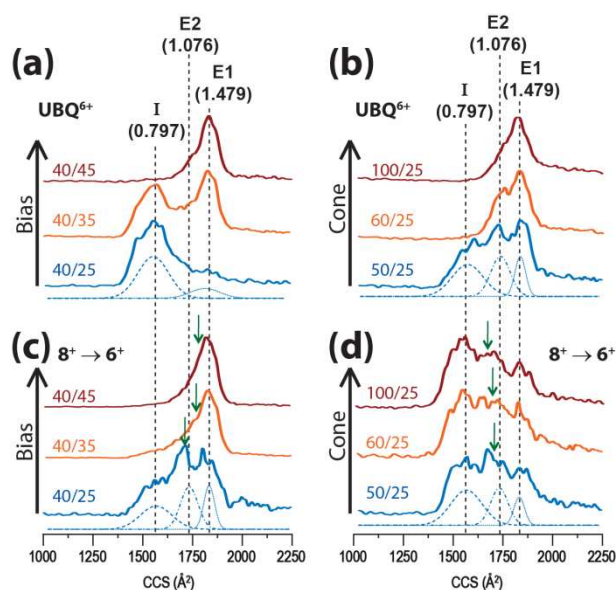


Figure 3. Collision cross sections for 6+ ubiquitin formed by either (a, b) electro spray ionization, or (c, d) charge reduction of ESI-generated $[M+8H]^{8+}$ by using ETD. Time axes of arrival time distributions were converted to CCS as described in [16]. Data shown in panels (a) and (c) were acquired using a sampling cone voltage of 40 V and a trap DC bias of either 25 (blue), 35 (orange), or 45 V (red). In panels (b) and (d), the bias was kept constant at 25 V and a sampling cone voltage of 50 (blue), 60 (orange), or 100 V (red) was applied. Colored text in panels indicates (cone voltage)/(bias voltage) for each trace. Gaussian components used in deconvolution of the lowest-energy (blue) trace in each panel are shown at the bottom at half-intensity. Values in parentheses are optimized apparent PTR/ETnoD ratios for each of these components, as described in the text. Weighted average CCS values (used to generate Figure 2) are indicated with green arrows in panels (c) and (d).

References

- [1] Syka, J.E., Coon, J.J., Schroeder, M.J., Shabanowitz, J., Hunt, D.F.: Peptide and protein sequence analysis by electron transfer dissociation mass spectrometry, *Proc Natl Acad Sci U S A* **101**, 9528-9533(2004)
- [2] Zhurov, K.O., Fornelli, L., Wodrich, M.D., Laskay, U.A., Tsybin, Y.O.: Principles of electron capture and transfer dissociation mass spectrometry applied to peptide and protein structure analysis, *Chem Soc Rev* **42**, 5014-5030(2013)
- [3] Pitteri, S.J., McLuckey, S.A.: Recent developments in the ion/ion chemistry of high-mass multiply charged ions, *Mass Spectrom Rev* **24**, 931-958(2005)
- [4] Abzalimov, R.R., Kaltashov, I.A.: Electrospray ionization mass spectrometry of highly heterogeneous protein systems: protein ion charge state assignment via incomplete charge reduction, *Anal Chem* **82**, 7523-7526(2010)
- [5] Lermyte, F., Williams, J.P., Brown, J.M., Martin, E.M., Sobott, F.: Extensive Charge Reduction and Dissociation of Intact Protein Complexes Following Electron Transfer on a Quadrupole-Ion Mobility-Time-of-Flight MS, *J Am Soc Mass Spectrom* **26**, 1068-1076(2015)
- [6] Laszlo, K.J., Bush, M.F.: Analysis of Native-Like Proteins and Protein Complexes Using Cation to Anion Proton Transfer Reactions (CAPTR), *J Am Soc Mass Spectr* **26**, 2152-2161(2015)
- [7] Lermyte, F., Łącki, M.K., Valkenborg, D., Baggerman, G., Gambin, A., Sobott, F.: Understanding reaction pathways in top-down ETD by dissecting isotope distributions: A mammoth task, *Int J Mass Spectrom* **390**, 146-154(2015)
- [8] Yao, C., Turecek, F.: Hypervalent ammonium radicals. Competitive N-C and N-H bond dissociations in methyl ammonium and ethyl ammonium, *Phys Chem Chem Phys* **7**, 912-920(2005)
- [9] Chakraborty, T., Holm, A.I., Hvelplund, P., Nielsen, S.B., Pouilly, J.C., Worm, E.S., Williams, E.R.: On the survival of peptide cations after electron capture: role of internal hydrogen bonding and microsolvation, *J Am Soc Mass Spectrom* **17**, 1675-1680(2006)
- [10] O'Connor, P.B., Lin, C., Cournoyer, J.J., Pittman, J.L., Belyayev, M., Budnik, B.A.: Long-lived electron capture dissociation product ions experience radical migration via hydrogen abstraction, *J Am Soc Mass Spectrom* **17**, 576-585(2006)
- [11] Turecek, F., Chen, X., Hao, C.: Where does the electron go? Electron distribution and reactivity of peptide cation radicals formed by electron transfer in the gas phase, *J Am Chem Soc* **130**, 8818-8833(2008)
- [12] Gunawardena, H.P., He, M., Chrisman, P.A., Pitteri, S.J., Hogan, J.M., Hodges, B.D., McLuckey, S.A.: Electron transfer versus proton transfer in gas-phase ion/ion reactions of polyprotonated peptides, *J Am Chem Soc* **127**, 12627-12639(2005)
- [13] Williams, J.P., Pringle, S., Richardson, K., Gethings, L., Vissers, J.P., De Cecco, M., Houel, S., Chakraborty, A.B., Yu, Y.Q., Chen, W., Brown, J.M.: Characterisation of glycoproteins using a quadrupole time-of-flight mass spectrometer configured for electron transfer dissociation, *Rapid communications in mass spectrometry : RCM* **27**, 2383-2390(2013)
- [14] Valentine, S.J., Counterman, A.E., Clemmer, D.E.: Conformer-dependent proton-transfer reactions of ubiquitin ions, *J Am Soc Mass Spectr* **8**, 954-961(1997)
- [15] Loo, R.R.O., Winger, B.E., Smith, R.D.: Proton transfer reaction studies of multiply charged proteins in a high mass-to-charge ratio quadrupole mass spectrometer, *J Am Soc Mass Spectrom* **5**, 1064-1071(1994)
- [16] Ruotolo, B.T., Benesch, J.L., Sandercock, A.M., Hyung, S.J., Robinson, C.V.: Ion mobility-mass spectrometry analysis of large protein complexes, *Nat Protoc* **3**, 1139-1152(2008)
- [17] Bush, M.F., Hall, Z., Giles, K., Hoyes, J., Robinson, C.V., Ruotolo, B.T.: Collision Cross Sections of Proteins and Their Complexes: A Calibration Framework and Database for Gas-Phase Structural Biology, *Anal Chem* **82**, 9557-9565(2010)
- [18] Williams, J.P., Brown, J.M., Campuzano, I., Sadler, P.J.: Identifying drug metallation sites on peptides using electron transfer dissociation (ETD), collision induced dissociation (CID) and ion mobility-mass spectrometry (IM-MS), *Chem Commun* **46**, 5458-5460(2010)

- [19] Lermyte, F., Verschueren, T., Brown, J.M., Williams, J.P., Valkenburg, D., Sobott, F.: Characterization of top-down ETD in a travelling-wave ion guide, *Methods* **89**, 22-29(2015)
- [20] Lermyte, F., Sobott, F.: Electron transfer dissociation provides higher-order structural information of native and partially unfolded protein complexes, *Proteomics* **15**, 2813-2822(2015)
- [21] Lossel, P., Snijder, J., Heck, A.J.: Boundaries of mass resolution in native mass spectrometry, *J Am Soc Mass Spectrom* **25**, 906-917(2014)
- [22] Ruotolo, B.T., Benesch, J.L.P., Sandercock, A.M., Hyung, S.J., Robinson, C.V.: Ion mobility-mass spectrometry analysis of large protein complexes, *Nat Protoc* **3**, 1139-1152(2008)
- [23] Zhao, Q., Soyk, M.W., Schieffer, G.M., Fuhrer, K., Gonin, M.M., Houk, R.S., Badman, E.R.: An Ion Trap-Ion Mobility-Time of Flight Mass Spectrometer with Three Ion Sources for Ion/Ion Reactions, *J Am Soc Mass Spectr* **20**, 1549-1561(2009)
- [24] Chen, S.H., Russell, D.H.: How Closely Related Are Conformations of Protein Ions Sampled by IM-MS to Native Solution Structures?, *J Am Soc Mass Spectr* **26**, 1433-1443(2015)
- [25] Scalf, M., Westphall, M.S., Krause, J., Kaufman, S.L., Smith, L.M.: Controlling charge states of large ions, *Science* **283**, 194-197(1999)
- [26] Scalf, M., Westphall, M.S., Smith, L.M.: Charge reduction electrospray mass spectrometry, *Anal Chem* **72**, 52-60(2000)
- [27] Prentice, B.M., McLuckey, S.A.: Gas-phase ion/ion reactions of peptides and proteins: acid/base, redox, and covalent chemistries, *Chem Commun* **49**, 947-965(2013)
- [28] Robb, D.B., Brown, J.M., Morris, M., Blades, M.W.: Method of atmospheric pressure charge stripping for electrospray ionization mass spectrometry and its application for the analysis of large poly(ethylene glycol)s, *Anal Chem* **86**, 9644-9652(2014)
- [29] Pagel, K., Hyung, S.J., Ruotolo, B.T., Robinson, C.V.: Alternate Dissociation Pathways Identified in Charge-Reduced Protein Complex Ions, *Anal Chem* **82**, 5363-5372(2010)
- [30] Bornschein, R.E., Hyung, S.J., Ruotolo, B.T.: Ion Mobility-Mass Spectrometry Reveals Conformational Changes in Charge Reduced Multiprotein Complexes, *J Am Soc Mass Spectr* **22**, 1690-1698(2011)
- [31] Campuzano, I., Schnier, P.: Coupling electrospray corona discharge, charge reduction and ion mobility mass spectrometry: From peptides to large macromolecular protein complexes, *Int J Ion Mobil Spec* **16**, 51-60(2013)
- [32] Bush, M.F., Campuzano, I.D., Robinson, C.V.: Ion mobility mass spectrometry of peptide ions: effects of drift gas and calibration strategies, *Anal Chem* **84**, 7124-7130(2012)
- [33] Revercomb, H.E., Mason, E.A.: Theory of Plasma Chromatography Gaseous Electrophoresis - Review, *Anal Chem* **47**, 970-983(1975)
- [34] Wyttenbach, T., Bowers, M.T.: Structural Stability from Solution to the Gas Phase: Native Solution Structure of Ubiquitin Survives Analysis in a Solvent-Free Ion Mobility-Mass Spectrometry Environment, *J Phys Chem B* **115**, 12266-12275(2011)
- [35] Laszlo, K.J., Munger, E., Bush, M.F.: Effects of Charge State on the Structures of Protein Ions: Results from Cation to Anion Proton Transfer Reactions, *Proceedings of the 63rd ASMS Conference on Mass Spectrometry and Allied Topics*, St. Louis, MO, TP26: 473(2015)
- [36] Zhao, Q., Schieffer, G.M., Soyk, M.W., Anderson, T.J., Houk, R.S., Badman, E.R.: Effects of Ion/Ion Proton Transfer Reactions on Conformation of Gas-Phase Cytochrome c Ions, *J Am Soc Mass Spectr* **21**, 1208-1217(2010)
- [37] Zhang, Z., Browne, S.J., Vachet, R.W.: Exploring salt bridge structures of gas-phase protein ions using multiple stages of electron transfer and collision induced dissociation, *J Am Soc Mass Spectrom* **25**, 604-613(2014)
- [38] Breuker, K., Oh, H.B., Horn, D.M., Cerda, B.A., McLafferty, F.W.: Detailed unfolding and folding of gaseous ubiquitin ions characterized by electron capture dissociation, *J Am Chem Soc* **124**, 6407-6420(2002)
- [39] Zhang, H., Cui, W.D., Gross, M.L.: Native electrospray ionization and electron-capture dissociation for comparison of protein structure in solution and the gas phase, *Int J Mass Spectrom* **354**, 288-291(2013)

- [40] Borysik, A.J., Kovacs, D., Guharoy, M., Tompa, P.: Ensemble Methods Enable a New Definition for the Solution to Gas-Phase Transfer of Intrinsically Disordered Proteins, *J Am Chem Soc* **137**, 13807-13817(2015)
- [41] Warnke, S., von Helden, G., Pagel, K.: Protein Structure in the Gas Phase: The Influence of Side-Chain Microsolvation, *J Am Chem Soc* **135**, 1177-1180(2013)

Supplementary Information

To estimate the (apparent) branching ratio for the second ($7+ \rightarrow 6+$) charge reduction step, we make use of a simple stochastic model. As mentioned in the main text, this ratio is directly measurable for the first ($8+ \rightarrow 7+$) step. Consider a cascade of PTR and ETnoD reactions (as shown in Figure 1) that occur m and n times, respectively, to generate a charge-reduced ion. In our specific example – double charge reduction of an $[M+8H]^{8+}$ ubiquitin ion – obviously ($m + n = 2$), ($0 \leq m \leq 2$), and ($0 \leq n \leq 2$). The observed abundance (calculated using MassTodon) of each charge-reduced product is denoted as α_{mn} . Assuming the behavior of ions to be independent and defining the probability of PTR and ETnoD as P_{PTR} and P_{ETnoD} , respectively, the probability (L) of observing the information found in the spectrum is given by

$$L = \prod_{m,n}^{observed} [(P_{PTR})^m (P_{ETnoD})^n]^{\alpha_{mn}}$$

Treating the above expression as a function of unknown parameters, i.e. the two probabilities, P_{ETnoD} and P_{PTR} , we can calculate values for these parameters so as to maximize L . This general postulate, that the theoretically most probable events occur in nature, is referred to as the *Maximum Likelihood* principle and is commonly used in statistics. Taking into account that $P_{ETnoD} + P_{PTR} = 1$ for charge reduction (equivalent to our assumption that other charge reduction pathways besides PTR and ETnoD can be neglected), the maximization results in estimates

$$P_{PTR} = \frac{\sum_{m,n} m \alpha_{mn}}{\sum_{m,n} (m + n) \alpha_{mn}}$$

$$P_{ETnoD} = \frac{\sum_{m,n} n \alpha_{mn}}{\sum_{m,n} (m + n) \alpha_{mn}}$$

As such, the (average) PTR/ETnoD branching ratio is provided by

$$\frac{P_{PTR}}{P_{ETnoD}} = \frac{\sum_{m,n} m \alpha_{mn}}{\sum_{m,n} n \alpha_{mn}}$$

Specifically for two-step charge reduction ETD of an $[M+8H]^{8+}$ ion, and explicitly writing out product formulas in the indices of the α coefficients, this yields

$$\frac{P_{PTR}}{P_{ETnoD}} = \frac{2 \cdot \alpha_{[M+6H]^{6+}} + \alpha_{[M+7H]^{6+\bullet}}}{\alpha_{[M+7H]^{6+\bullet}} + 2 \cdot \alpha_{[M+8H]^{6+\bullet\bullet}}}$$

This formula yields optimized values for a two-step process, in which P_{PTR} and P_{ETnoD} for both steps are equal. From this average value, combined with the (directly measurable) ratio for the first ($8+ \rightarrow 7+$) reaction step, the branching ratio for the second ($7+ \rightarrow 6+$) charge reduction step can easily be calculated separately and this value is reported in the main text.

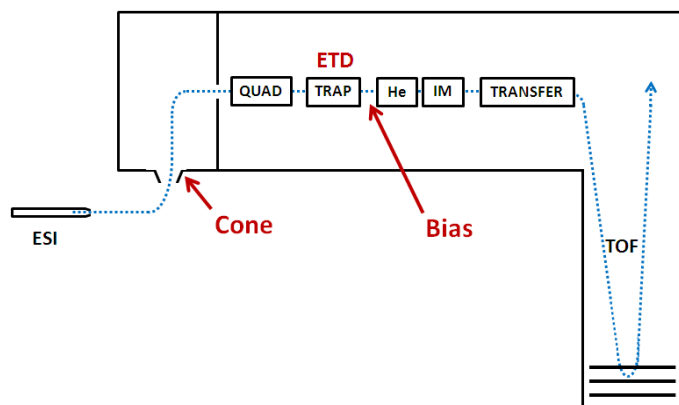


Figure S-1. Schematic overview of the Synapt G2 instrument used in this study, highlighting the location where sampling cone and trap DC bias voltages are applied, as well as where the ETD reaction occurs. The ion path is shown as a blue dotted line.

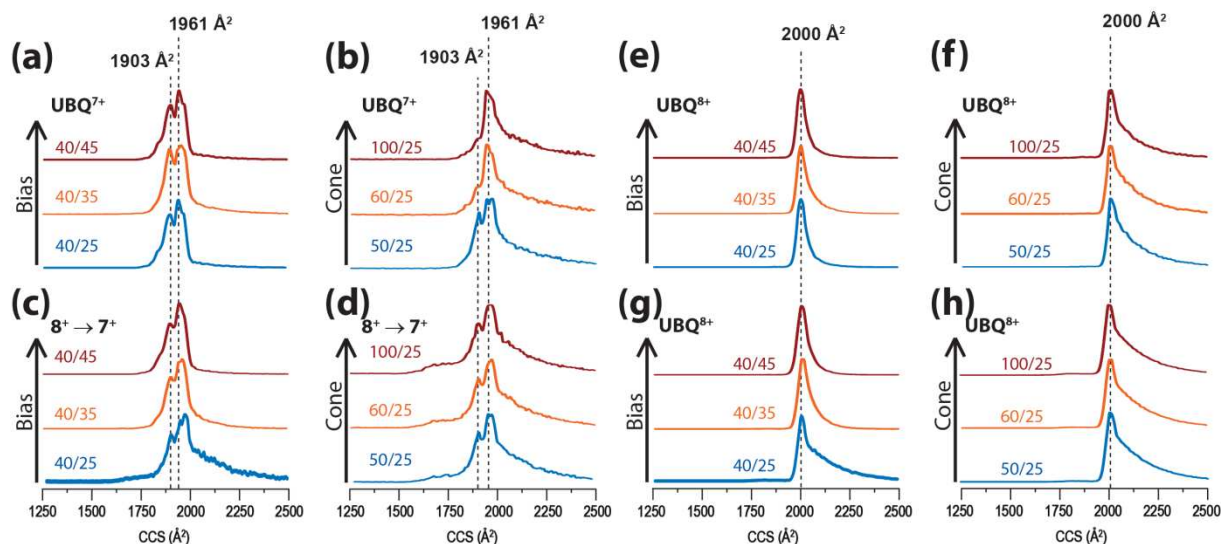


Figure S-2. Collision cross-sections for (a, b, c, d) 7+ and (e, f, g, h) 8+ ubiquitin formed by either (a, b, e, f) electrospray ionization, or (c, d, g, h) under ETD charge reduction conditions. The $[(M+8H)]^{8+}$ ion was selected in the quadrupole in all charge-reduction experiments, so note that the CCS distributions shown in panels (g) and (h) are not actually the result of charge reduction. Traces in panels (a, c, e, g) were acquired using a sampling cone voltage of 40 V and a trap DC bias of either (blue) 25, (orange) 35, or (red) 45 V. In panels (b, d, f, h), the bias was kept constant at 25 V and a sampling cone voltage of (blue) 60, (orange) 80, or (red) 100 V was applied.

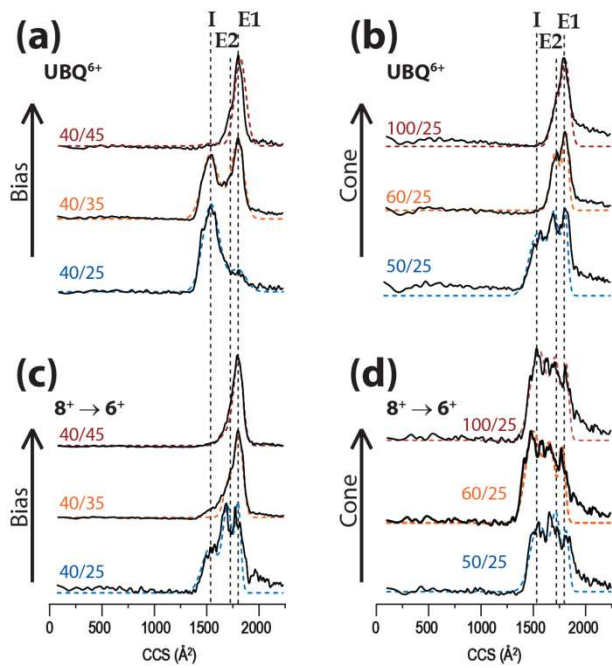


Figure S-3. Comparison of experimental spectra (black, solid lines) shown in Figure 3 of the main text to the result of deconvolution into Gaussian components corresponding to the *I*(ntermediate), *E*(xtended)-1, and *E*(xtended)-2 conformational states of ubiquitin (color, dotted lines).

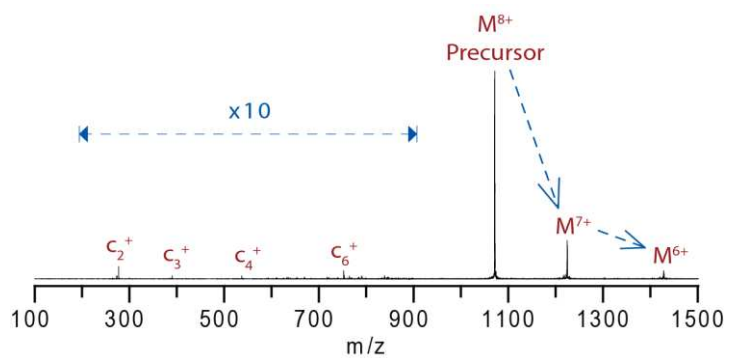


Figure S-4. Representative crETD spectrum of $[M+8H]^{8+}$ ubiquitin, showing the extent of charge reduction and fragment release (sampling cone 40 V, trap DC bias 25 V; 10-fold magnification in the range between 200 – 900 m/z).

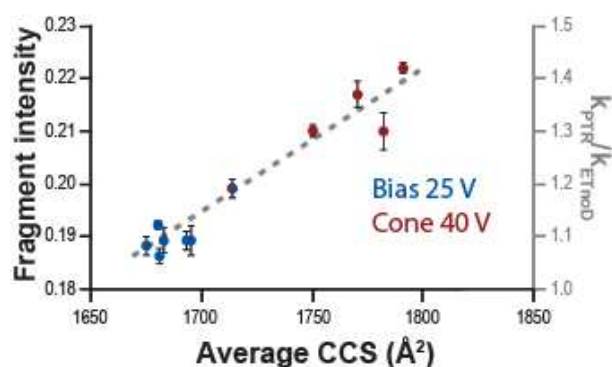


Figure S-5. Relative total ETD fragment intensity (axis on left-hand side) observed under the eleven sets of (cone/bias) voltages displayed in Figure 2 of the main text versus average collision cross-section for the corresponding 6+ charge-reduced state. Correlation between apparent PTR/ETNoD branching ratio (axis on right-hand side and shaded in gray) and CCS is displayed here as a gray dashed line to illustrate that fragmentation efficiency follows a similar trend. This is in agreement with our hypothesis that the conformation-dependent shift in isotope distribution is primarily due to differences in efficiency of fragment release. As in Figure 2, blue dots indicate experiments in which the bias voltage was held constant at 25 V (variable sampling cone voltage); red dots indicate a constant cone voltage of 40 V, with variable trap DC bias.